Geological Society of America
Special Paper 385
2005

GPS results from Puerto Rico and the Virgin Islands: Constraints on tectonic setting and rates of active faulting

Pamela E. Jansma
Glen S. Mattioli
Department of Geosciences, University of Arkansas, Fayetteville, Arkansas 72701, USA

ABSTRACT

Puerto Rico and the northern Virgin Islands define the eastern terminus of the Greater Antilles, which extend eastward from offshore eastern Central America to the Lesser Antilles volcanic arc and mark the boundary between the Caribbean and North America plates. In Hispaniola, Puerto Rico, and the northern Virgin Islands, the Puerto Rico trench and the Muertos trough define the northern and southern limits of the plate boundary zone, respectively. Three microplates lie within the boundary zone: (1) the Gonave in the west; (2) the Hispaniola in the center; and (3) the Puerto Rico–northern Virgin Islands in the east. Results from Global Positioning System (GPS) geodesy conducted in the region since 1994 confirm the presence of an independently translating Puerto Rico–northern Virgin Islands microplate whose motion is 2.6 ± 2.0 mm/yr toward N82.5°W ± 34° (95%) with respect to the Caribbean. Geodetic data are consistent with east-west extension of several mm/yr from eastern Hispaniola to the eastern Virgin Islands. Extension increases westward with the most, 5 ± 3 mm/yr, accommodated in the Mona rift, confirming earlier GPS geodetic results. East-west extension of 3 ± 2 mm/yr also is observed across the island of Puerto Rico, consistent with composite focal mechanisms and regional epicentral distributions. Although the loci of extension are not known, similarity of GPS-derived velocities among sites in eastern Puerto Rico suggests the active structures lie west of the San Juan metropolitan area. Reactivation of the Great Northern and Southern Puerto Rico fault zones as oblique normal faults with right-lateral slip is a possibility. East-west extension of 2 ± 1 mm/yr also must exist between eastern Puerto Rico and Virgin Gorda, which likely is attached to the Caribbean plate. These extensional belts allow eastward transfer of slip between North America and the Caribbean from the southern part of the plate boundary zone in the west to the northern segment in the east. Motions along or across any of the individual subaerial structures of Puerto Rico are ≤2 mm/yr. The Lajas Valley in the southwest, where microseismicity is greatest, is the locus of highest permissible on-land deformation. Northwest-southeast to east-west extension of 2 ± 1 mm/yr is also observed across the Anegada Passage.

Keywords: microplate tectonics, Caribbean, GPS geodesy, extension.

Jansma, P.E., and G.S. Mattioli, G.S., 2005, GPS results from Puerto Rico and the Virgin Islands: Constraints on tectonic setting and rates of active faulting, *in* Mann, P., ed., Active tectonics and seismic hazards of Puerto Rico, the Virgin Islands, and offshore areas: Geological Society of America Special Paper 385, p. 13–30.

INTRODUCTION

One of the fundamental questions concerning lithospheric behavior in zones of active tectonics is how relative motion between blocks or plates is accommodated. Is motion taken up along a few major faults or narrow belts of deformation separating discrete crustal blocks, or is strain broadly distributed throughout the deforming region as similar displacements occur on many closely spaced faults of comparable size? The two end members have different implications for seismic hazard. Larger earthquakes within narrow zones are likely to occur in the former, whereas smaller events over a broad region are more probable in the latter. Which end member more closely characterizes Puerto Rico and the northern Virgin Islands has long been controversial, i.e., do Puerto Rico and the northern Virgin Islands define a discrete, rigid block within the North America–Caribbean plate boundary within which little motion occurs, or do several faults capable of accommodating significant displacement cross the region? Recent results from Global Positioning System (GPS) geodesy provide upper bounds on the potential intrablock displacement.

Puerto Rico and the northern Virgin Islands define the eastern terminus of the Greater Antilles, which extend eastward from offshore eastern Central America to the Lesser Antilles volcanic arc and mark the boundary between the Caribbean and North America plates. Tectonic models for the northern Caribbean (e.g., Byrne et al., 1985; Mann et al., 1995) propose active microplates within the boundary zone on the basis of geologic and earthquake evidence. Seismicity along the EW-trending boundary between the North America and Caribbean plates is consistent with evolution of the boundary zone from a relatively simple set of transform faults in the west to a more complex deformation zone ~250 km wide in the east (Fig. 1A). Motion along the predominantly east-west striking major structures of the northern Caribbean is primarily left-lateral. In the west, the Swan and Oriente transform faults define the EW-trending Cayman trough and bound the short (~100 km), NS-trending Mid-Cayman spreading center (Fig. 1B). In Hispaniola, Puerto Rico, and the Virgin Islands, the Puerto Rico trench and the Muertos trough define the northern and southern limits of the plate boundary zone, respectively. Three microplates lie within this diffuse boundary zone (Fig. 1B): (1) the Gonave in the west (Mann et al., 1995); (2) the Hispaniola in the center (Byrne et al., 1985); and (3) the Puerto Rico–northern Virgin Islands in the east (Masson and Scanlon, 1991). Such a microplate model assumes that nearly all of the deformation associated with North America–Caribbean motion is concentrated along the faults that bound the three rigid blocks: the Oriente, Septentrional, Enriquillo-Plantain Garden, and Anegada faults; the Muertos trough and North Hispaniola deformed belt; and the Mona rift faults northwest of Puerto Rico (Fig. 1).

Recent results from GPS geodesy support the presence of an independently translating Puerto Rico–northern Virgin Islands microplate within the northeastern Caribbean (Jansma et al., 2000) with ~85% of the relative motion occurring between the Puerto Rico–northern Virgin Islands and North America and ~15% between the Puerto Rico–northern Virgin Islands and the Caribbean. (This distribution of interplate slip is our current best estimate, given that rigorous quantitative modeling is not yet completed, and potential elastic strain accumulation along the Puerto Rico trench has not been considered). The geodetic data are not consistent with models that advocate either counterclockwise rotation of the Puerto Rico–northern Virgin Islands about a nearby vertical axis (Masson and Scanlon, 1991; Reid et al., 1991) or eastward tectonic escape of the block within the Caribbean–North America plate boundary zone (Jany et al., 1987). Because velocities of the Puerto Rico–northern Virgin Islands microplate with respect to the Caribbean plate are small and the errors were significant, both as a consequence of the paucity of data for a Caribbean reference frame and the geographically restricted GPS network, Jansma et al. (2000) were limited in their interpretation of interplate deformation along the Puerto Rico–northern Virgin Islands–Caribbean boundary and intrablock deformation of the Puerto Rico–northern Virgin Islands. In this paper, we update the analysis of Jansma et al. (2000) with the inclusion of additional geodetic data from both existing and new continuous and campaign GPS sites in the Puerto Rico–northern Virgin Islands block. We also use ITRF00 (International Terrestrial Frame 2000) and an improved Caribbean reference frame (DeMets et al., 2000, and 2002, personal commun.). Our objectives are to refine the velocity of the Puerto Rico–northern Virgin Islands block with respect to the Caribbean plate, to constrain maximum permissible displacements along potentially active faults on the island of Puerto Rico and immediately offshore, and to examine potential diffuse extension between the Virgin Islands and eastern Puerto Rico.

TECTONIC SETTING OF PUERTO RICO AND THE VIRGIN ISLANDS

Hundreds of earthquakes per year occur within and around Puerto Rico and the Virgin Islands (Fig. 1). The majority of events are small and located offshore. Several large events have occurred during historic time, including the 1916, 1918, and 1943 Mona Passage earthquakes (Ms = 7.2, 7.3, and 7.5, respectively), the 1867 Anegada earthquake (Ms = 7.3), the 1787 Puerto Rico trench earthquake (M = 7.5?) and the 1670 San German earthquake (M = 6.5?) (Pacheco and Sykes, 1992). Noting the concentration of both current seismicity and historic events offshore (Fig. 1C), several workers proposed a rigid Puerto Rico–northern Virgin Islands block in the northeastern corner of the Caribbean (Byrne et al., 1985; Masson and Scanlon, 1991).

The EW-striking Puerto Rico trench and Muertos trough define the northern and southern limits of the Puerto Rico–northern Virgin Islands, respectively (Fig. 1). Both are characterized by diffuse zones of earthquakes that dip below the island of Puerto Rico (McCann and Pennington, 1990; McCann, 2002), consistent with subduction of Atlantic lithosphere below northern Puerto Rico and Caribbean lithosphere below the southwestern coast of the island. Interaction of the two slabs at depth has

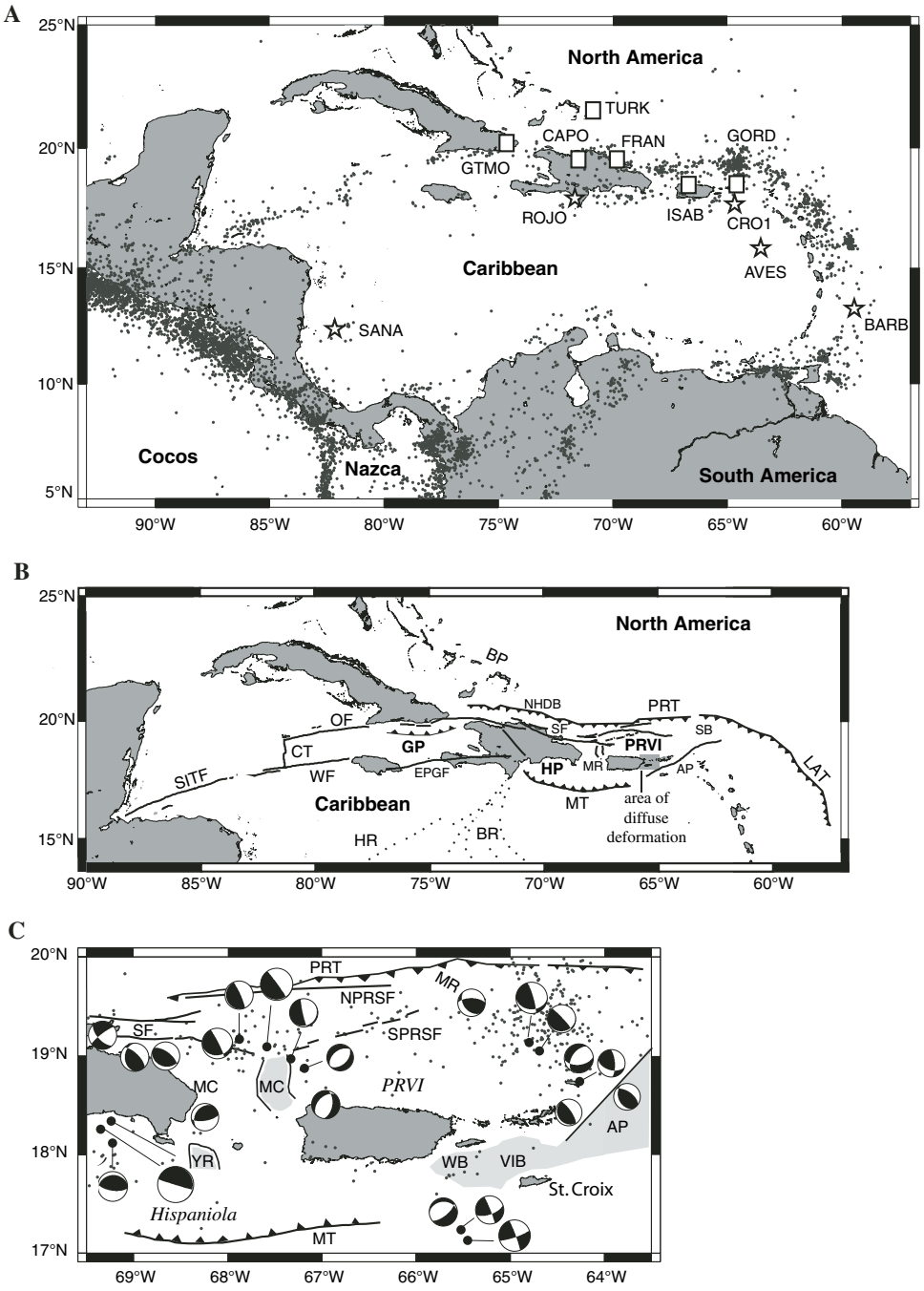

Figure 1. (A) Map of Caribbean plate and regional seismicity. Epicenters are for earthquakes above depths of 60 km with magnitudes >3.5 from 1 January 1967 until 28 April 1999 (U.S. Geological Survey). The five GPS sites used to constrain Caribbean reference frame are plotted as stars: SANA—San Andres Island; ROJO—Cabo Rojo, Dominican Republic; CRO1—St. Croix, U.S. Virgin Islands; AVES—Aves Island; and BARB—Barbados. Original CANAPE Global Positioning System sites are ROJO and CRO1 plus the squares: CAPO—Capotillo, Dominican Republic; FRAN—Cabo Frances Viejo, Dominican Republic; GORD—Virgin Gorda; GTMO—Guantanamo Bay, Cuba; ISAB—Isabela, Puerto Rico; and TURK—Grand Turk, Turks and Caicos. (B) Map of northern Caribbean plate boundary showing microplates and structures. AP—Anegada Passage; BP—Bahamas Platform; BR—Beata Ridge; CT—Cayman trough spreading center; EPGF—Enriquillo-Plantain Garden fault; GP—Gonave platelet; HP—Hispaniola platelet; HR—Hess Rise; LAT—Lesser Antilles Trench; MR—Mona Rift; MT—Muertos trough; NHDB—North Hispaniola deformed belt; OF—Oriente fault; PRT—Puerto Rico Trench; PRVI—Puerto Rico–Virgin Islands block; SB—Sombrero Basin; SITF—Swan Islands transform fault; SF—Septentrional fault; WF—Walton fault. (C) Focal mechanisms for depth <35 km for eastern Hispaniola, Puerto Rico, and Virgin Islands. Sources are the Harvard CMT (Centroid-Moment Tensor) catalogue, the Puerto Rico Seismic Network, Deng and Sykes (1995), and Molnar and Sykes (1969). Dots are USGS epicenters for earthquakes above depths of 60 km with magnitudes >3.5 from 1 January 1967 until 28 April 1999 (USGS). Abbreviations as in Figure 1B. MC—Mona Canyon; NPRSF—North Puerto Rico Slope fault; SPRSF—South Puerto Rico Slope fault; VIB—Virgin Islands Basin; WB—Whiting Basin; YR—Yuma Rift.

been postulated (Dolan and Wald, 1998; Dolan et al., 1998) with resultant arching of the island of Puerto Rico about an EW-oriented axis above (van Gestel et al., 1998). The Puerto Rico trench lies ~100 km offshore and reaches a water depth >8 km. Water depth in the Muertos trough is ~5 km. GPS-derived velocities of western Puerto Rico with respect to North America are consistent with oblique convergence across the western Puerto Rico trench (Jansma et al., 2000). Geologic evidence to support convergence includes earthquake slip vectors and low-angle thrusts imaged in seismic profiles (Sykes et al., 1982; Deng and Sykes, 1995; Larue and Ryan, 1998). The Puerto Rico trench and additional mapped offshore faults between the north coast of Puerto Rico and the Puerto Rico trench, such as the South Puerto Rico Slope fault (Grindlay et al., 1997) accommodate ~85% of the current highly oblique North America–Caribbean relative plate motion. The remaining 15% must be taken up along onland faults in Puerto Rico or along the Muertos trough. These results are preliminary and await confirmation by quantitative models of slip distribution. GPS-derived velocities of Puerto Rico with respect to the Caribbean are small, making interpretations from 1999 and

earlier geodetic data alone tenuous. Evidence for ongoing deformation along the western Muertos trough includes seismicity and the existence of an accretionary prism along the lower slope south of southeastern Hispaniola and southwestern Puerto Rico along which 40 km of underthrusting is thought to have occurred (Ladd et al., 1977; Ladd and Watkins, 1978; Byrne et al., 1985; Larue and Ryan, 1990; McCann and Pennington, 1990; Masson and Scanlon, 1991; Deng and Sykes, 1995). The accretionary prism narrows eastward along the southern boundary of the Puerto Rico–northern Virgin Islands microplate and disappears near 65°W, southwest of St. Croix (Mauffret and Jany, 1990; Masson and Scanlon, 1991), implying an eastward decrease in normal convergence across the Muertos trough.

The Mona passage, which bounds the Puerto Rico–northern Virgin Islands microplate to the west, contains the NS-trending Mona rift in the north and the similarly oriented Yuma rift in the south (Figs. 1 and 2). The Mona rift formed as a result of east-west extension between Puerto Rico and Hispaniola during the last few million years (Larue and Ryan, 1990, 1998; van Gestel et al., 1998). The 1918 earthquake (Ms = 7.3) in the Mona rift likely occurred along a NS-trending normal fault (Mercado and McCann, 1998) and indicates extension in the Mona rift is ongoing. Focal mechanisms of other historic and recent events offshore northwestern Puerto Rico are consistent with normal faulting along NNE-striking planes (Fig. 1C) (Doser et al., this volume). The kinematics of the Yuma rift are not well constrained, and thus the nature of the boundary between the Puerto Rico–northern Virgin Islands and Hispaniola microplates south of the Mona rift is unclear.

The eastern boundary of the Puerto Rico–northern Virgin Islands block is marked by the ENE-trending Anegada passage, which connects the Neogene Virgin Island and Whiting basins in the southwest with the Sombrero basin in the northeast (Fig. 1). Transtension is likely across the Anegada passage, which is dominated by northeast-southwest–striking and east-west–striking faults with a significant extensional component (Jany et al., 1987; Holcombe et al., 1989; Masson and Scanlon, 1991). Normal displacements along the major faults decrease southwestward to the Muertos trough from more than 4 km to zero over a distance of 50 km, implying rapidly decreasing extension westward (Masson and Scanlon, 1991). North of the Virgin Islands, where most large historic earthquakes have occurred (Murphy and McCann, 1979; Frankel et al., 1980; McCann, 1985; Doser et al., this volume), focal mechanisms record a combination of reverse and sinistral motion along roughly east-west–striking faults, reflecting ENE–directed relative motion of the Caribbean with respect to North America.

ON-LAND FAULTING ON PUERTO RICO

Most studies of on-land faults in Puerto Rico have focused primarily on structures that cut Tertiary and older rocks (Glover and Mattson, 1960; Glover, 1971; Erikson et al., 1990, 1991). Prior to the work of Prentice and Mann (this volume) and Mann et al. (this volume) documentation of features that offset Quaternary units has been limited (e.g., McCann, 1985; Meltzer et al., 1995), leaving most workers to model Puerto Rico as a rigid block (e.g., Masson and Scanlon, 1991). Shallow microseismic-

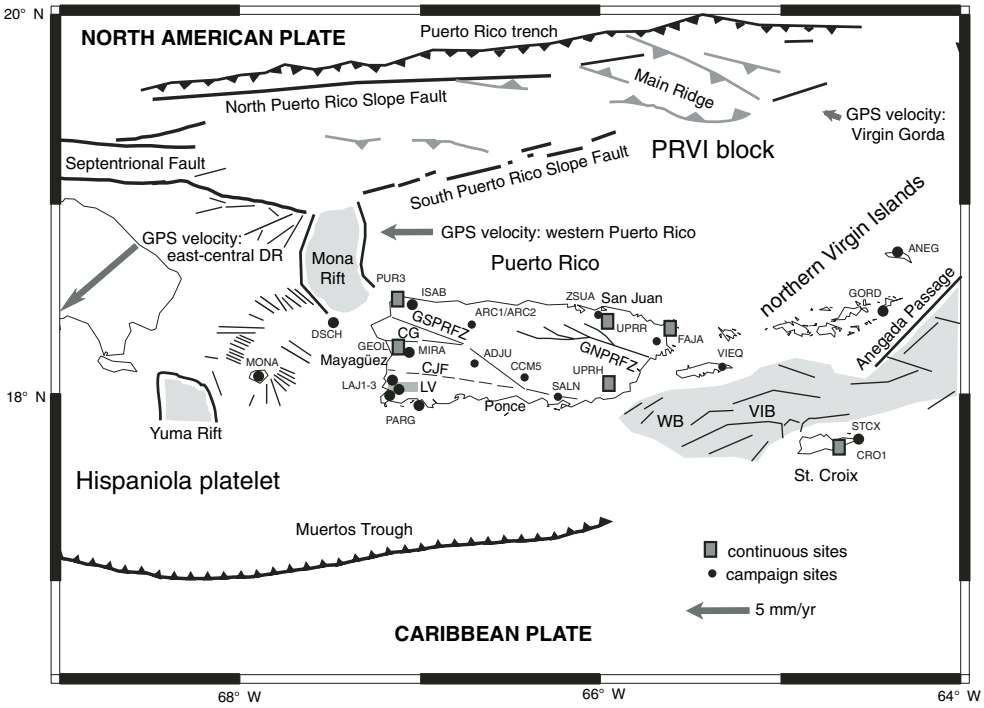

Figure 2. Current mixed-mode Global Positioning System (GPS) geodetic network in the northeastern Caribbean. GNPRFZ—Great Northern Puerto Rico fault zone; GSPRFZ—Great Southern Puerto Rico fault zone; CG—Cerro Goden fault; CJF—postulated Cordillera-Joyuda faults; LV—Lajas Valley (medium gray shaded rectangle in southwestern Puerto Rico). Major offshore structures also are shown. Light gray shaded regions are zones of inferred extension. WB—Whiting Basin; VIB—Virgin Islands Basin. Arrow in Dominican Republic is GPS-derived velocity relative to the fixed Caribbean for central Hispaniola, south of Septentrional fault. Arrow north of the island of Puerto Rico is average GPS-derived velocity relative to the Caribbean for sites in western Puerto Rico. Arrow north of the northern Virgin Islands is GPS-derived velocity relative to the Caribbean for site in Virgin Gorda. Length of arrow in lower left corresponds to 5 mm/yr for scale. Error ellipses are not shown for clarity.

ity does occur onshore, but the historic record is consistent with major events limited to the offshore region (McCann, 2002). The recognition of Quaternary displacements when coupled with observations of shallow seismicity in western Puerto Rico, however, appears to argue against truly rigid-block behavior. The important questions to be answered are: what are the permissible displacement rates along the mapped faults given the GPS geodetic results, do these rates agree with those derived from the geologic data, and are these rates consistent with significant and therefore possibly destructive earthquakes occurring along subaerial faults within the Puerto Rico–northern Virgin Islands microplate?

The highest levels of onshore seismicity are in the Lajas Valley (Asencio, 1980), an EW-trending feature in southwestern Puerto Rico, which continues offshore to the west and passes south of the southern termination of the Mona Canyon, where offshore faults are mapped (Fig. 2). Quaternary offsets along the southern edge of the Lajas Valley were interpreted from seismic reflection profiles (Meltzer et al., 1995; Meltzer, 1997), and active faulting was inferred from the "basin-and-range" style topography of the region (Joyce et al., 1987). Displacements along the EW-striking faults are inferred to be normal with components of strike-slip (Meltzer, 1997; Almy et al., 2000; Prentice et al., 2000). In addition, the island of Puerto Rico is traversed by two northwest-southeast striking fault zones: (1) the Great Northern Puerto Rico fault zone, and (2) the Great Southern Puerto Rico fault zone (Fig. 2). The fault zones were active during the Eocene and record predominantly thrust and left-lateral displacement in response to amalgamation of discrete island arc terranes at the leading edge of the Caribbean plate into the Puerto Rico–northern Virgin Islands microplate (Glover and Mattson, 1960; Glover, 1971; Erikson et al., 1990, 1991). Both the Great Northern Puerto Rico fault zone and the southern end of the Great Southern Puerto Rico fault zone are covered by little-deformed Neogene strata. The two fault zones, however, represent large areas of weakness within the Puerto Rico–northern Virgin Islands along which active displacements may be localized. Indeed, the southern end of the Great Southern Puerto Rico fault zone immediately offshore may cut and disturb Recent shelf sediments (McCann, 1985; J. Joyce, 2000, personal commun.). The projection of the northern end of the Great Southern Puerto Rico fault zone, which continues offshore into Mona Canyon, is subparallel to faults of similar orientation (NW-SE), which are seismically active (McCann, 1985; Joyce et al., 1987). In addition, an EW-striking splay of the Great Southern Puerto Rico fault zone, the Cerro Goden fault, cuts across to the west coast of Puerto Rico ~10 km north of the city of Mayagüez (Fig. 2). Whether Quaternary motion occurred along the Cerro Goden fault is unknown, although the offshore projection of the fault merges with other mapped structures that presumably are Quaternary in age. Lao-Davila et al. (2000) infer Recent displacement with components of normal motion and left-lateral strike-slip on the basis of offset stream drainages and terraces. Some workers have identified the surficial expressions of the Cordillera and Joyuda faults, which they argue may correspond to a WNW-ESE trend across southwestern Puerto Rico that is defined by a series of epicenters of small earthquakes that were recorded by the Puerto Rico Seismic Network in 1995 (J. Moya, 1999, personal commun.). Geological estimates for displacements along the fault are unconstrained.

PRIOR GPS RESULTS FOR PUERTO RICO AND THE NORTHERN VIRGIN ISLANDS

Jansma et al. (2000) provided a detailed discussion and interpretation of GPS geodetic data collected in the Puerto Rico–northern Virgin Islands microplate from 1994 until 1999. With the exception of two sites (ZSUA in San Juan and GORD in Virgin Gorda), the network consisted of stations in western Puerto Rico. Their results, therefore, emphasized the western half of the island and are summarized below.

To assess if Puerto Rico was attached to the Caribbean plate, Jansma et al. (2000) compared the predicted velocity of the Caribbean with respect to the North America plate at the longitude of western Puerto Rico from the model of DeMets et al. (2000) against the velocity of western Puerto Rico relative to North America derived from GPS geodetic data. The predicted and GPS-derived velocities of the Caribbean with respect to North America for western Puerto Rico are 19.4 ± 1.2 mm/yr toward N79°E ± 3° (1σ) and 16.9 ± 1.1 mm/yr with an azimuth of N68°E ± 3 (1σ), respectively, with the latter slightly slower and more northerly than that for Caribbean–North America plate motion as a whole. Thus nearly 85% of the relative motion between the Caribbean and North America plates is accommodated offshore northern Puerto Rico. Relative motion of western Puerto Rico with respect to the Caribbean as constrained by GPS geodesy through 1999 is 2.4 ± 1.4 mm/yr to the west (Jansma et al., 2000). The slow velocity of Puerto Rico with respect to the Caribbean has led some authors to assume that Puerto Rico is part of the Caribbean plate and to include sites in Puerto Rico in the formulation of the Caribbean reference frame (Weber et al., 2001). Although this interpretation was permissible given the errors associated with the geodetic data included in the inversion of the Euler pole, we believe that Puerto Rico is a discrete microplate. The current geodetic data set allows us to infer this unequivocally (see below). Additional compelling evidence is seismicity associated with the Muertos trough, which defines a pattern consistent with overriding of Caribbean lithosphere by southwestern Puerto Rico (Byrne et al., 1985; Dolan and Wald, 1998; McCann et al., this volume).

To assess whether the Puerto Rico–northern Virgin Islands block is rigid, Jansma et al. (2000) used the methodology of Ward (1990) to examine the dispersion of geodetic velocities about predictions of an angular velocity that best-fits those velocities. The results were only applicable to western Puerto Rico where the majority of sites were located. The average rate misfit to the 14 horizontal velocity components of the seven sites that were included (ARC1, GEOL, ISAB, MIRA, PARG, PUR3 AND ZSUA) was 1.2 mm/yr, with only two velocity components misfit by more than 2 mm/yr and one misfit at a level exceeding

one standard deviation. The data were fit within their estimated uncertainties of 1–3 mm/yr. The approximate upper bound on the level of internal deformation of western Puerto Rico thus is 1–3 mm/yr. Velocity uncertainties were on the order of several mm/yr for GPS sites in eastern Puerto Rico.

In contrast to western Puerto Rico where GPS velocities of the Puerto Rico–northern Virgin Islands microplate with respect to the Caribbean are significant above error, the GPS-derived velocity at Virgin Gorda (GORD) at the eastern end of a presumed Puerto Rico–northern Virgin Islands block (Fig. 2) is zero within error to that predicted for the Caribbean plate at that location (DeMets et al., 2000; Jansma et al., 2000). The eastern Virgin Islands, therefore, may be attached to the Caribbean plate, implying no displacement along or across the eastern Anegada passage and a zone of EW extension of a few millimeters per year between Virgin Gorda and western Puerto Rico (Fig. 2). The limited time series and geographic distribution of the network made these interpretations only tentative in Jansma et al. (2000). We reexamine these conclusions here with the additional geodetic data from new campaign and continuous sites, additional occupations for preexisting campaign sites and the accumulation of two more years of data for continuous GPS (CGPS) sites.

The GPS-derived velocities relative to the Caribbean plate were consistent with W to SW motion of Hispaniola within the plate boundary zone at a rate faster than that of Puerto Rico, yielding EW extension of 5 ± 3 mm/yr across the NS-trending Mona passage (Fig. 2). The large velocity of Hispaniola with respect to the Caribbean (and, therefore, lower relative motion with respect to North America) within the plate boundary zone likely reflects collision with the Bahama Bank (Mann et al., 1995), a carbonate platform that extends northwest from the northern Dominican Republic to offshore Florida (Fig. 1B). In contrast, Puerto Rico has bypassed the collision and translates eastward with respect to North America at nearly the Caribbean–North America plate rate.

THE CARIBBEAN REFERENCE FRAME

One of the critical issues for GPS geodesy in the northeastern Caribbean is the development and potential limitations of a Caribbean reference frame. The published version is that of DeMets et al. (2000), which uses GPS-derived velocities from Aves Island (AVES) in the east, San Andres Island (SANA) in the west, St. Croix (CRO1) in the U.S. Virgin Islands, and Cabo Rojo (ROJO) in the southern Dominican Republic (Fig. 1). To supplement the limited geodetic data, azimuths of the eastern Swan Islands transform fault also are included to constrain Caribbean motion. CRO1 is the only continuous site of the original four and has been recording data since late 1995. Time series for the other sites range from 4 to 8 years. An updated version of the reference frame incorporates the CGPS site in Barbados (BARB, Fig. 1) and is the one we use in this paper (DeMets et al., 2000, and 2002, personal commun.). The best-fit angular velocity for the five Caribbean GPS sites yields an average residual velocity of 1.5 mm/yr. Another realization of the Caribbean reference frame by Weber et al. (2001) uses Barbados (BARB, Fig. 1) and also includes Puerto Rico (ISAB, Fig. 1). As we will show below, the latter likely sits on a separate tectonic block within the plate boundary zone and sites there will introduce increased uncertainties.

NEW GPS DATA ACQUISITION

GPS measurements were first collected in the northeastern Caribbean in 1986 at six locations (Fig. 1) (Dixon et al., 1991), which were reoccupied subsequently as part of CANAPE (Caribbean–North American Plate Experiment) in 1994. The original sites were: Grand Turk (TURK), Turks and Caicos; Guantanamo (GTMO), Cuba; Cabo Rojo (ROJO), Capotillo (CAPO), and Cabo Frances Viejo (FRAN) in the Dominican Republic, St. Croix (STCX), U.S. Virgin Islands, and Isabela (ISAB), Puerto Rico (Dixon et al., 1991). The network was densified during CANAPE and each subsequent year (for details, see Dixon et al., 1998; Jansma et al., 2000; Calais et al., 2002; Mann et al., 2002). Since 1994, measurements have been made on subsets of the entire network each year. A permanent IGS (International GPS Service) station was established in St. Croix in 1995 (CRO1) and a vector tie to the original 1986 site, STCX, was established (Dixon et al., 1998), which extended the time series by nearly a decade and therefore improved the CRO1 velocity estimate.

The GPS network in Puerto Rico and the Virgin Islands (Fig. 2) consists of the original 1994 CANAPE locations (ISAB, PARG, and GORD) plus campaign sites MIRA (Miradero-Mayagüez), ZSUA (San Juan), MONA (Mona island), DSCH (Desecheo island), ADJU (Adjuntas), ARC2 (Arecibo), CCM5 (Ponce), FAJA (Fajardo), LAJ1, LAJ2, and LAJ3 (Lajas Valley), SALN (Salinas), VIEQ (Vieques), and ANEG (Anegada, British Virgin Islands) and continuous sites GEOL in Mayagüez, FAJA in Fajardo, UPRR in Rio Piedras, and UPRH in Humacao operated by the Department of Geosciences, University of Arkansas, and PUR3 in Aguadilla maintained by the U.S. Coast Guard.

Details of the campaign observations from 1994 to 1999 can be found in Jansma et al. (2000) and will not be repeated here. All campaign observations after 1999 were obtained with the following hardware: Trimble 4000 SSi 12-channel, dual-frequency code-phase receivers and Dorn-Margolin type choke ring antennae. Data were collected using either 0.5 m spike mounts or standard tripod and/or rotating optical plummet setups at a 30 s observation epoch and 10° elevation mask. An individual campaign occupation usually obtained between 10–24 h of continuous data for 2–3 consecutive observation days. The descriptions of the continuous sites remain unchanged from that reported in Jansma et al. (2000).

Previously, we chose to report and analyze CGPS data from PUR3, GEOL, and CRO1. Here we include data from FAJA, a CGPS site in northeastern Puerto Rico for which over two years of observations now exist. Two additional new CGPS stations, UPRH (University of Puerto Rico, Humacao) and UPRR (University of Puerto Rico, Rio Piedras) had been operating for approximately one year at the time of our analysis for this report.

Accordingly, these sites have not yet accumulated enough data to merit serious interpretation.

DATA ANALYSIS

Data from continuous sites PUR3, GEOL, FAJA, and CRO1 (Fig. 3) and campaign sites ISAB, PARG, ADJN, ARC2, ZSUA, SALN, and GORD (Fig. 4) are considered in this paper. Although several additional campaign sites have been installed on the Puerto Rico–northern Virgin Islands block since 2000, most have only had initial occupations completed to date. Others that have had a second occupation have only 1.5–1.8 yr between observations, making estimates of their velocities too uncertain at this time. Data from a total of 11 sites are reported here.

Data analysis procedures have changed slightly from those reported in Jansma et al. (2000) and only a brief description and the significant departures will be reviewed here. All data were processed as free-network point positions using GIPSY-OASISII (version 2.5.8a) (Lichten, 1990; Zumberge et al., 1997). Free-network solutions were transformed, scaled, and rotated into

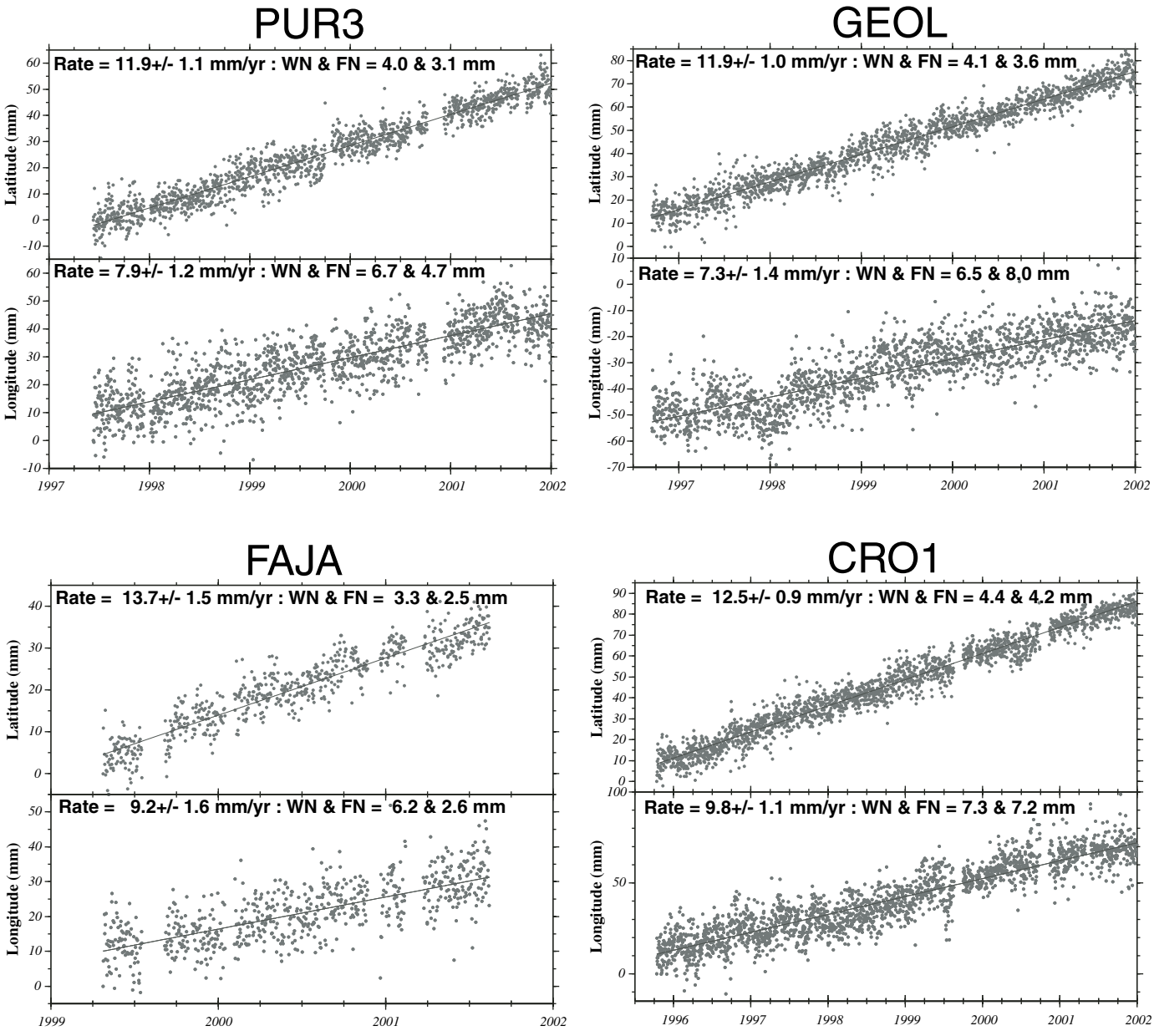

Figure 3. Global Positioning System station latitude and longitude coordinate time series for continuous stations PUR3, GEOL, FAJA, and CRO1. Daily point positions are in ITRF00 (International terrestrial reference frame, 2000). Formal solution errors are not shown for clarity. Note correlated noise among the three sites. WN—white noise; FN—flicker noise.

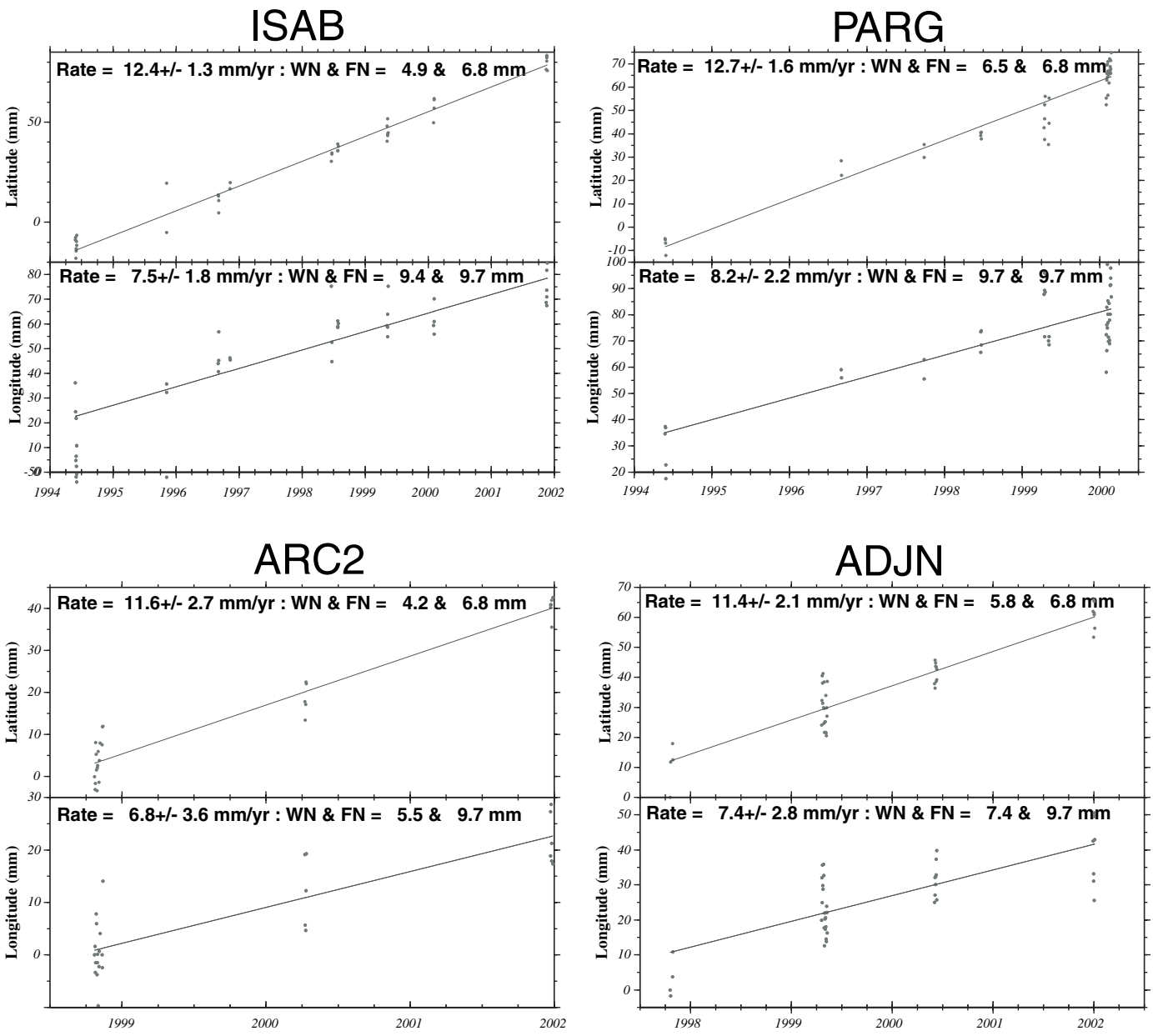

ITRF00 (the current realization of the International Terrestrial Reference Frame, epoch 2000) using x-files from the Jet Propulsion Laboratory (JPL; Blewitt et al., 1992; Heflin et al. 1992). All processing used final, precise non-fiducial orbit, earth-orientation, and GPS clock files from JPL (300 s epoch). Time series velocity errors were calculated using the formulation of Mao et al. (1999), which includes both colored (time-correlated) and white noise contributions and an assumed estimate of √2 mm/yr of random monument noise at each site. Scaled formal error estimates for individual site positions are not shown on the time series plots as their utility is recognized as limited. Component site velocities were calculated in ITRF00 using post-processing software modules, which allow estimation of component offsets along with estimates of velocities in a rapid and internally consistent way that includes the full-covariance of each daily site position in the analysis.

After obtaining an ITRF00 velocity for the latitude, longitude, and radial component and their associated errors, final velocities and errors in the Caribbean reference frame were calculated using the current best-fit model for Caribbean motion with respect to the ITRF00. Caribbean fixed velocities include the full covariance of the individual sites velocities and the predicted motion of the Caribbean plate at that location (DeMets et al., 2000, and 2002, personal commun.). Velocities and their

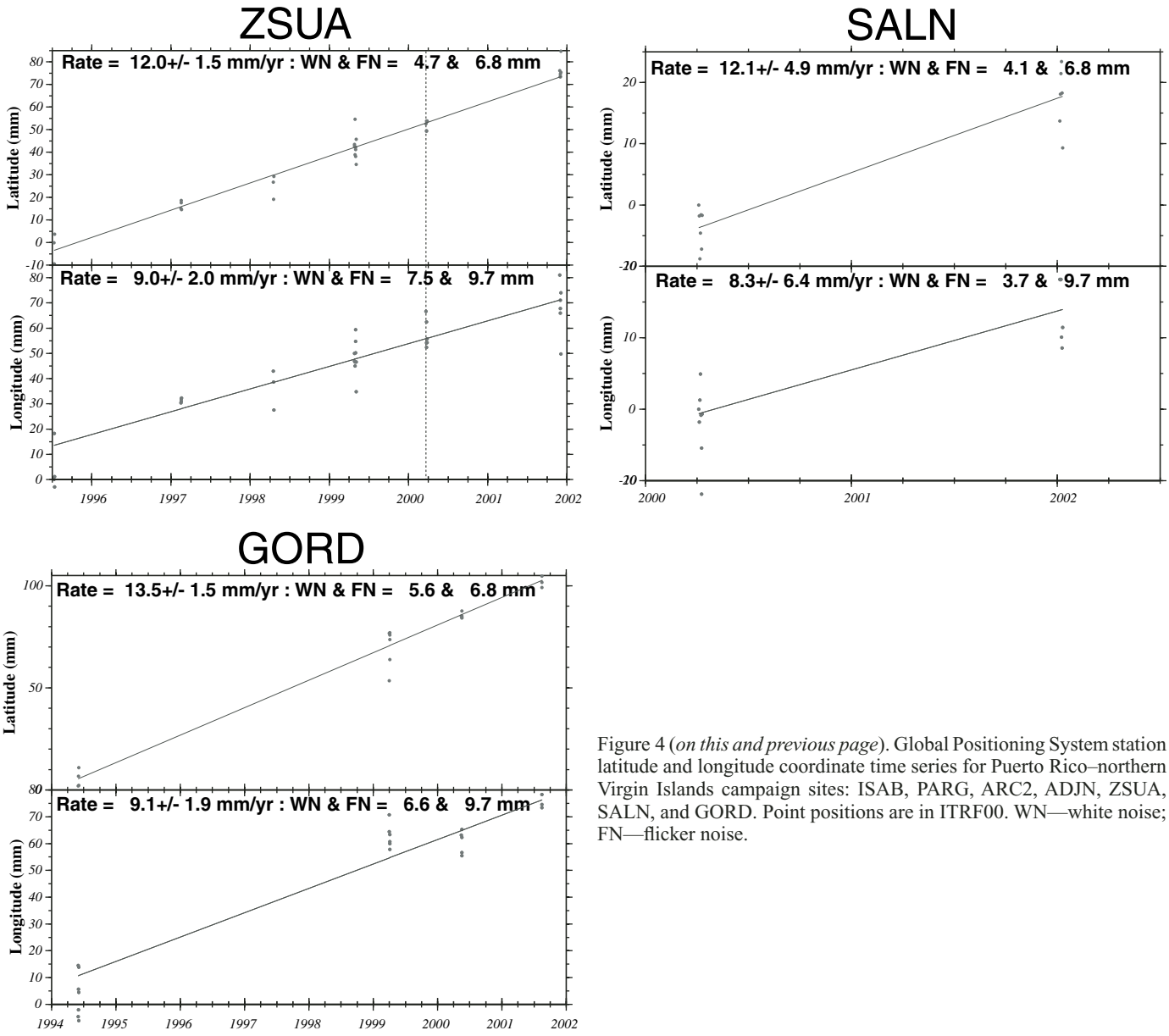

Figure 4 (*on this and previous page*). Global Positioning System station latitude and longitude coordinate time series for Puerto Rico–northern Virgin Islands campaign sites: ISAB, PARG, ARC2, ADJN, ZSUA, SALN, and GORD. Point positions are in ITRF00. WN—white noise; FN—flicker noise.

errors are shown with respect to ITRF00 and the Caribbean reference frame in Table 1. Error ellipses in Figure 5A are 1σ and include both the error of the site time series and the Caribbean reference frame formulation.

In addition to the point positions and velocities derived from them, baseline lengths and components (north, east, and up) were determined to evaluate the internal deformation of the Puerto Rico–northern Virgin Islands block. The derived baseline data have been calculated from the ITRF00 site positions by geometrical differencing using standard GIPSY-OASISII routines to obtain relative changes in station position of the second station with respect to fixed position of the first station. Phase ambiguities were not resolved and therefore the baseline lengths and component velocities are simply a recasting of the absolute point position results described above into a fixed-site reference frame. Such estimates, although useful, can potentially yield spurious results because of spatially correlated noise and unmodeled monument motion (Langbein and Johnson, 1997). No attempt was made during most campaign occupations to assure that several other sites were operating simultaneously, which limits the available data for this type of analysis primarily to the four CGPS sites (PUR3, GEOL, FAJA, and CRO1), and the PARG and ISAB campaign sites, which fortuitously have several synchronous observations over a six year period. The Caribbean-fixed and Puerto Rico–northern Virgin Islands site-fixed velocities and their errors are discussed in detail below.

TABLE 1. VELOCITIES OF GPS SITES IN PUERTO RICO AND THE VIRGIN ISLANDS IN ITRF2000 AND WITH RESPECT TO THE STABLE CARIBBEAN

	Latitude north	Longitude east	Time span (years)	Velocity north (ITRF2000) (mm/yr)	Velocity east (ITRF2000) (mm/yr)	Velocity north (Caribbean) (mm/yr)	Velocity east (Caribbean) (mm/yr)
ADJN	18.17	292.20	4.211	11.4 ± 2.1	7.4 ± 2.8	–0.6 ± 2.2	–3.2 ± 2.9
ARC2	18.34	293.25	3.181	11.6 ± 2.7	6.8 ± 3.6	–0.4 ± 2.7	–3.8 ± 3.7
CRO1	17.76	295.42	6.216	12.5 ± 0.9	9.8 ± 1.1	–0.3 ± 1.5	–1.2 ± 1.4
FAJA	18.38	294.38	2.301	13.7 ± 1.5	9.2 ± 1.6	1.4 ± 1.7	–1.4 ± 1.8
GEOL	18.21	292.86	5.290	11.9 ± 1.0	7.3 ± 1.4	0.1 ± 1.2	–3.3 ± 1.6
GORD	18.43	295.56	7.214	13.5 ± 1.5	9.1 ± 1.9	0.6 ± 1.6	–1.6 ± 2.1
ISAB	18.47	292.95	7.488	12.4 ± 1.3	7.5 ± 1.8	0.5 ± 1.4	–3.0 ± 2.0
PARG	17.97	292.96	5.750	12.7 ± 1.6	8.2 ± 2.2	0.8 ± 1.7	–2.5 ± 1.7
PUR3	18.46	292.93	4.556	11.9 ± 1.1	7.9 ± 1.2	0.1 ± 1.2	–2.6 ± 1.5
SALN	18.03	293.77	1.768	12.1 ± 4.9	8.3 ± 6.4	–0.1 ± 5.0	–2.4 ± 6.5
ZSUA	18.43	294.01	6.406	12.0 ± 1.5	9.0 ± 2.0	–0.3 ± 1.6	–1.6 ± 2.2

Note: For definition of stable Caribbean, see text. Uncertainties are 1σ and include white noise, flicker noise, and monument error. ITRF2000—International terrestrial reference frame—2000.

GPS-DERIVED VELOCITIES AND BASELINES FOR PUERTO RICO AND THE VIRGIN ISLANDS

In our discussion of GPS-derived velocities and baselines, we separate the island of Puerto Rico from the neighboring Virgin Islands to the east. Our reasoning is that the potential attachment of Virgin Gorda (GORD) to the Caribbean plate requires small relative motion between the eastern Virgin Islands and eastern Puerto Rico. To assess whether the island of Puerto Rico and the Virgin Islands as a whole are each rigid, we examine GPS-derived velocities of sites in Puerto Rico and the Virgin Islands relative to the Caribbean. To constrain the permissible upper limits for displacement rates along active faults in Puerto Rico, we include in our analysis calculated component velocities relative to continuous GPS sites that cross major structures: PUR3-GEOL; PUR3-PARG; PUR3-FAJA; GEOL-FAJA; FAJA-CRO1; and PUR3-CRO1. PARG, a campaign site, also is used to create baselines that cross the seismically active Lajas Valley (PARG-PUR3; PARG-GEOL).

Velocities of Puerto Rico and the Virgin Islands Relative to the Caribbean Plate: Implications for a Separate Puerto Rico–Northern Virgin Islands Microplate

GPS-derived velocities relative to the Caribbean for the Puerto Rico–northern Virgin Islands block appear consistent with a linear increase in velocity from near zero (1.7 ± 2.1 mm/yr) at Virgin Gorda (GORD) in the east to ~3 mm/yr (3.0 ± 0.3 mm/yr mean and standard deviation of the average of five sites) toward the west along the west coast of Puerto Rico (Fig. 5A, Table 1). To assess whether motion of the Puerto Rico–northern Virgin Islands microplate with respect to the Caribbean was significant, we tested for the existence of a separate microplate using the F-ratio test of Stein and Gordon (1984). This method compares the weighted least-squares fits of models that use two angular velocities (six parameters) and one angular velocity (three parameters), respectively, to fit a set of kinematic observations, in our case, five Caribbean and 15 Puerto Rico–northern Virgin Islands sites. The F-test is insensitive to systematic overestimates or underestimates of velocity uncertainties, an important consideration with GPS velocities. We undertook a similar analysis in Jansma et al. (2000) using the geodetic data collected between 1994 and 1998. Our previous attempt resulted in significance of a separate Puerto Rico–northern Virgin Islands block only at the 80% confidence level. We estimated that an additional two years of data would be required before the GPS-derived velocities would be sufficiently precise to detect motion of the Puerto Rico–northern Virgin Islands relative to the Caribbean of a few mm/yr at the 95% confidence level. The F-test is defined here as:

$$F = \frac{\left[\chi^2_{(2\ \text{plates})} - \chi^2_{(1\ \text{plate})}\right]/3}{\chi^2_{(2\ \text{plates})}/\nu}$$

where χ^2 is defined as the weighted root mean square misfit (chi-squared) of the kinematic model to the GPS site velocities and ν represents the number of degrees of freedom ($N - p$), which in this case is 40 – 6 or 34.

Fitting the Puerto Rico–northern Virgin Islands and Caribbean velocities with a single angular velocity gives a summed weighted least-squares misfit of 20.78. Fitting the two sets of velocities with separate angular velocities gives a summed misfit of 13.16. The improvement in fit from the 2-plate model, which stems from using three additional adjustable parameters, gives F = 6.56, which is significant at the 99.9% confidence level for 3 versus 34 degrees of freedom. The inclusion of the additional data thus constrains the unequivocal existence of a Puerto Rico–northern Virgin Islands microplate within the northeastern Caribbean. This conclusion is robust despite the still significant error in the individual time series of Puerto Rico–northern Virgin Islands

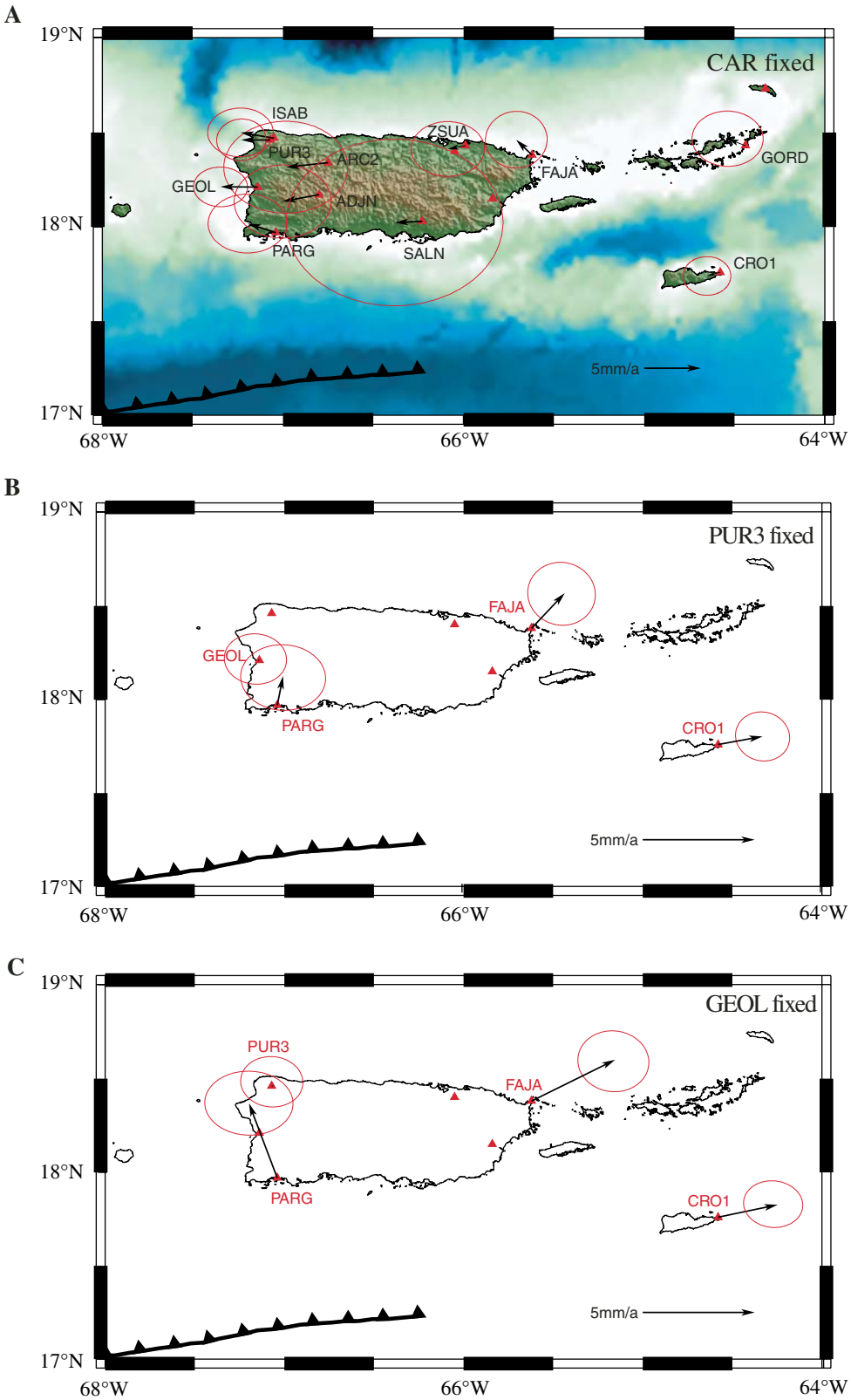

Figure 5. (A) Velocities relative to Caribbean reference frame. Confidence ellipses are 1σ. Heavy black line with triangles offshore south of Puerto Rico represents the Muertos trough. (B) Velocities relative to fixed GEOL. For magnitude of changes along baselines, see Table 2. (C) Velocities relative to fixed PUR3. Table 2 lists velocities and 1σ for sites. Note that calculated 1σ errors were determined by propagating errors from the ITRF2000 time series component errors and likely are overestimates; therefore, error ellipses shown have been scaled to 0.5 1σ.

TABLE 2. BASELINE VELOCITY COMPONENTS FOR SELECTED PAIRS OF GPS SITES IN PUERTO RICO AND THE VIRGIN ISLANDS.

Baseline	Fixed site	Velocity north (mm/yr)	Velocity east (mm/yr)	Correlation coefficient
GEOL-PUR3	GEOL	0.02 ± 1.49	0.10 ± 1.84	–0.0328
GEOL-PARG	GEOL	3.34 ± 1.89	–1.26 ± 2.61	–0.0123
GEOL-FAJA	GEOL	1.85 ± 1.80	3.74 ± 2.10	–0.0368
GEOL-CRO1	GEOL	0.56 ± 1.38	2.66 ± 1.75	–0.0485
PUR3-PARG	PUR3	1.31 ± 1.94	–0.26 ± 2.51	–0.0274
PUR3-FAJA	PUR3	1.58 ± 1.86	1.49 ± 2.00	–0.0426
PUR3-CRO1	PUR3	0.36 ± 1.45	1.99 ± 1.60	–0.0538
FAJA-CR01	FAJA	–2.13 ± 1.77	0.96 ± 1.92	–0.0508
ISAB-PARG	ISAB	0.47 ± 2.06	–1.07 ± 2.84	–0.0027

Note: Changes are expressed in terms of velocity north and velocity east in mm/yr. Stated error is 1σ propagated from International terrestrial reference frame—2000 time series component errors without any provision for common mode errors. It is likely that these stated uncertainties substantially overestimate the real uncertainties.

sites. We note that site velocities for all 15 Puerto Rico–northern Virgin Islands sites are included in our analysis, despite the fact that four of these sites (ARC1, MIRA, UPRR, and ZSUB) are not reported in Table 1 because their time series component errors remain too large for meaningful geologic interpretation. The total contribution of these site velocities to the final best fit (2-plate) kinematic model is 0.36 out of 6, or only 6%, however, and thus they have little impact on the final model. Their low contribution arises because these site velocities are more imprecise than other sites located nearby. Additional kinematic modeling and further details will be reported elsewhere.

Velocities of Puerto Rico and the Virgin Islands Relative to the Caribbean Plate: Implications for Internal Puerto Rico–Northern Virgin Islands Microplate Deformation

Although all Puerto Rico–northern Virgin Islands velocities are similar within error, raising the possibility that no deformation occurs across the microplate, we believe that the systematic pattern of the velocities across the Puerto Rico–northern Virgin Islands block suggests that the small differences are likely real, although they are close to the limits of detection in the current geodetic data. The observed residual velocities are not likely a result of bias in the location of the Caribbean Euler pole because the location of the pole is much farther away than the distance between the sites in the Puerto Rico–northern Virgin Islands microplate. Changes in the location or rotation rate for the Caribbean would cause a systematic shift in the observed Puerto Rico–northern Virgin Islands residual velocities, but would not eliminate the observed differences among the sites within the Puerto Rico–northern Virgin Islands block. The new observations support earlier interpretations that the Puerto Rico–northern Virgin Islands block may be attached to the Caribbean plate at GORD on its eastern end, requiring east-west extension across Puerto Rico and the western Virgin Islands (Jansma et al., 2000). The preliminary results were based on only two epochs (1994 and 1999) of data at GORD. The new data set includes additional epochs at GORD in 2000 and 2001, such that the time series reported here spans seven years (Fig. 4 and Table 1). The inclusion of data from FAJA in the northeastern corner of Puerto Rico and from SALN in south-central Puerto Rico also strengthens this conclusion: the GPS-derived velocities of FAJA and SALN (average of 2.2 ± 0.3 mm/yr) relative to the Caribbean are faster than that of GORD (1.72 ± 2.1 mm/yr), but slower than that of GEOL, PUR3, PARG, ADJN, and ARC2 (average of 3.0 ± 0.3 mm/yr). The magnitude of the velocity of FAJA also is similar to the magnitude of that at ZSUA, ~35 km to the west. The velocity azimuths, however, vary by ~45°.

Comparison of the GPS-derived velocities relative to the Caribbean at GORD, SALN, and FAJA provides important constraints for the neotectonics of the Anegada passage. At the longitude of GORD, where the velocity is zero within error, little if any motion occurs across the Anegada passage. The possibility does exist that CRO1 and GORD velocities are affected by strain accumulation along a locked, fast-slipping, eastern Anegada passage fault. We believe this is unlikely, however, because of the similarity of CRO1's velocity with the other rigid Caribbean sites (AVES, SANA, ROJO, BARB) (DeMets et al., 2000). We note that CRO1 is closer to the Anegada passage faults than GORD and therefore should be more affected by any possible strain accumulation along these structures. Low levels of microseismicity south of the eastern Virgin Islands (Frankel et al., 1980) also support little motion between GORD and CRO1. To the west, however, where microseismicity is greater and motions of FAJA and SALN with respect to the Caribbean are toward the northwest and west, respectively (Fig. 5A), displacement across the northeast-trending structures of the Whiting and Virgin Island basins must have an extensional component, a conclusion supported by evidence of normal faulting documented in seismic profiles acquired in the Anegada passage (Jany et al., 1987; Holcombe et

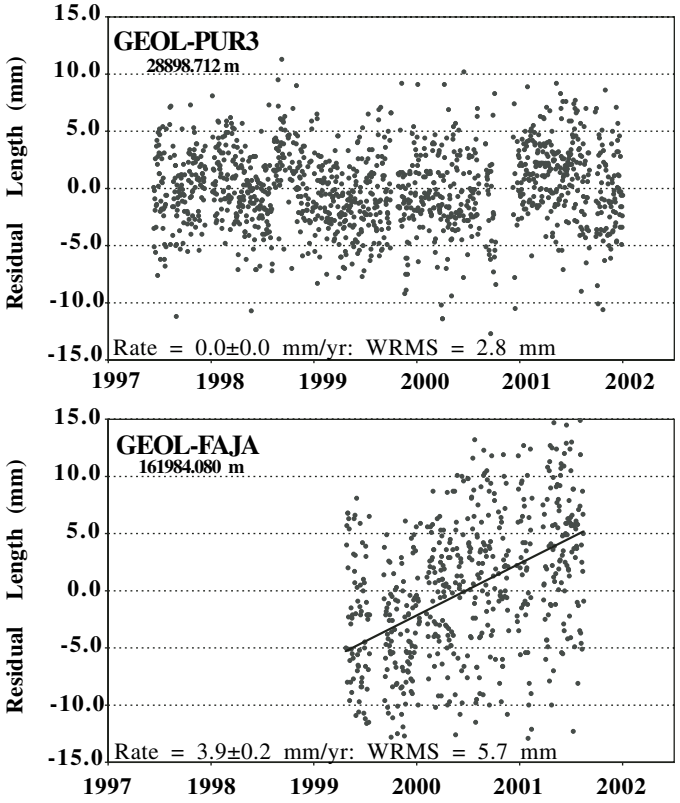

Figure 6. Evolution of residual baseline length between continuous sites PUR3 and GEOL (upper) and GEOL and FAJA (lower). Rate of change of baseline length between PUR3 and GEOL is 0.0 ± 0.0 mm/yr. Motion transverse to the baseline of –0.1 ± 0.1 also occurs. WRMS (weighted root mean square) is 2.8 mm. Median baseline length is 28898.712 m. Rate of change of baseline length between GEOL and FAJA is 3.9 ± 0.2 mm/yr. Motion transverse to the baseline of 1.4 ± 0.1 also occurs. WRMS is 5.7 mm. Median baseline length is 161984.080 m. Stated error is 1σ formal error with white noise only and no provision for monument noise.

al., 1989; Masson and Scanlon, 1991). The change from near zero motion at GORD to 2.0 ± 1.8 mm/yr relative to the Caribbean at FAJA (Fig. 5A, Table 1) requires a small component of northwest-southeast to east-west extension between the eastern Virgin Islands and eastern Puerto Rico. The northwest-oriented velocity of FAJA relative to the Caribbean yields northwest-southeast extension across the Anegada passage at the longitude of 65°W, whereas the west-directed velocity relative to the Caribbean of SALN produces near east-west extension across the Whiting and Virgin Islands basins south of Vieques. The westward motion of western Puerto Rico relative to the Caribbean of 3.0 ± 0.3 mm/yr (average of five sites) implies a component of left-lateral strike-slip motion along either the east-west–trending Muertos trough or offshore faults south of Puerto Rico at the longitude of western and central Puerto Rico. Up to 2 mm/yr of convergence also is permitted along the Muertos trough within error (Fig. 5A).

Puerto Rico–Northern Virgin Islands–Fixed Component Velocities and Baseline Evolution for Selected Site Pairs in Puerto Rico

Although the GPS-derived velocities of sites in Puerto Rico and the Virgin Islands relative to the Caribbean are essential to constrain the kinematics of the Puerto Rico–northern Virgin Islands microplate, the 1σ uncertainties associated with the individual site velocities frequently exceed geologically based estimates of slip rates along those faults. To assess whether the small differences among the GPS-derived velocities for sites in Puerto Rico were geologically significant, we examined the evolution of component velocities and baseline lengths between several pairs of CGPS stations in the northeastern Caribbean. The campaign sites, PARG and ISAB, also were included in our analysis. The CGPS sites were selected because they have the longest time series, which generally should minimize the error associated with the calculations, although as we will discuss below, CGPS data also may be biased. PARG and ISAB were included to provide baseline coverage of structures in southwest Puerto Rico. Relative velocity components (north, east, and up) (Table 2) and length were calculated among the CGPS sites and the ISAB and PARG campaign sites holding either GEOL, PUR3, or ISAB fixed in the ISAB-PARG baseline. Vectors shown in Figures 5B and 5C were determined by holding the ITRF00 position of one site fixed as a reference, GEOL in the case of the upper diagram, and determining the relative change for the north and east components for the other sites. Derived time series of the baseline components were then used to calculate component velocities. The full covariance for each component velocity in ITRF00 was included in the calculation of the standard deviation in fixed site component velocities reported in Table 2. The estimated component velocity errors already included our estimate of white time-correlated and monument noise. They do not include any provision, however, for error reduction as a result of common-mode noise in the time series and therefore are likely to be larger than the real errors for these site pairs.

The derived residual baseline length change for GEOL-FAJA is 3.9 ± 0.2 mm/yr, for example, appears to be inconsistent with velocities reported in Table 1 in either the ITRF00 or Caribbean reference frame. Using the ITRF00 component velocities from Table 1, the square root of the sum of the squared differences for GEOL-FAJA is 2.4 ± 3.2 mm/yr rather than the 3.9 ± 0.2 mm/yr determined by the baseline evolution shown in Figure 6. In principle, the coordinate transformation whereby GEOL was held fixed should not have biased the calculated baseline length change, if the linear model and associated errors for the component velocities accurately represents the temporal evolution of the GEOL and FAJA point positions. This apparently was not the case here. The FAJA time series is much shorter and started much later than the GEOL time series. To test whether this affected our results, we have recalculated the GEOL component velocities using only position estimates overlapping in time with FAJA. The result is V_{north} = 11.6 ± 1.6 mm/yr and V_{east} = 5.2 ± 1.6 mm/

yr (2.31 yr from April 24, 1999, to August 15, 2001, relative to ITRF00). This is essentially the same in the north component, but substantially different in the east component (7.3 ± 1.4 and 5.2 ± 1.6 mm/yr for the full versus the abbreviated time series, respectively). The implication of this is that between April 1999 and August 2001, the GEOL site motion did not closely approximate its site velocity for the much longer 5.3 yr period. Using these rates for GEOL and recalculating the expected baseline rate of change as well as propagating the errors in the point position time series yields 4.2 ± 3.4 mm/yr for the motion of FAJA relative to fixed GEOL. The motion of FAJA relative to fixed GEOL can now be recast into baseline and transverse components changes for comparison with the baseline evolution diagram shown in Figure 6. The resulting V_{length} = 4.0 ± 3.1 mm/yr is now in excellent agreement with the 3.9 ± 0.2 calculated by solely fitting the baseline length residuals. Taking a very conservative approach, we can safely estimate that the baseline length change between FAJA and GEOL is between the 2.3 ± 3.0 and 4.0 ± 3.1 mm/yr estimates. In contrast, the PUR3-GEOL baseline length change of 0.0 ± 0.0 mm/yr shown in Figure 6 closely approximates the calculated difference based on the velocity time series of 0.1 ± 1.5 mm/yr. In this case, either long period noise does not affect this northeast-oriented baseline significantly or the 4.6 yr period over which we have calculated the velocities and residual baseline changes is sufficient to effectively average them out. Because of these considerations, real errors remain relatively large for the baseline estimates and care must be exercised in their interpretation. Nevertheless, we believe that an internally consistent tectonic model can be developed based upon both the point position estimates in the Caribbean fixed frame and the calculated baseline changes. This is presented below.

GEOLOGICAL AND TECTONIC IMPLICATIONS

From Northwestern to Southwestern Puerto Rico: Displacement across Subaerial Faults and Zone of High Microseismicity

To constrain the upper bounds of displacements along potentially active faults in western Puerto Rico, we examined two baselines: PUR3-GEOL, which extends generally north-south from the northwestern corner of the island to Mayagüez in the central western coast, and PUR3-PARG, which joins the northwestern and southwestern corners of Puerto Rico and crosses the seismically active Lajas Valley. PUR3-GEOL crosses the Great Southern Puerto Rico fault zone and the Cerro Goden fault (Fig. 2). The length of the baseline between PUR3 and GEOL has remained constant within error during the 4.5 yr interval for which we have data (Fig. 6) (Table 2). The total integrated displacement across the Great Southern Puerto Rico fault zone and the Cerro Goden fault, therefore, is less than the 0.0–1.6 mm/yr error estimated along the baseline.

In contrast, the length of the baseline between PUR3 and PARG has decreased 1.6 ± 0.3 mm/yr during the same time interval. (The baselines ISAB-PARG and GEOL-PARG yielded similar results.) The velocity of PARG relative to a fixed PUR3 is oriented NNE (Figs. 5B and 5C), a direction perpendicular to the major structures of the plate boundary and consistent with a component of convergence across the Caribbean-Puerto Rico boundary zone. Because PARG is a campaign site with only six epochs of observations, the errors associated with this baseline are larger than those between two continuous sites. Nevertheless, the implication is that deformation ≤2 mm/yr is likely across southwestern Puerto Rico, a scenario that is not unreasonable given the high microseismicity in the Lajas Valley (Asencio, 1980) (Fig. 2). The decrease in line length implies shortening between PARG and GEOL. East-west–trending faults that bound the Lajas Valley, therefore, likely have oblique-reverse motion. Because the degree of obliquity is small, the sense of the component of strike-slip displacement predicted along the edges of the Lajas Valley and the postulated Cordillera and Joyuda faults is highly sensitive to slight changes in the azimuth of the displacement between PUR3 and PARG and these remain uncertain. The sense implied by the baseline change, however, is right-lateral. Trenching across one of the bounding faults of the Lajas Valley revealed components of normal (valley-side down) and strike-slip displacement (Prentice and Mann, this volume). Because a three-dimensional excavation of channels and other features was not attempted, no quantitative estimate of the sense of fault offset could be determined. Almy et al. (2000) argued for components of normal motion and left-lateral strike-slip. Other evidence for normal faulting in southwestern Puerto Rico along east-west to northwest-southeast trends is cited from seismic reflection profiling of the Lajas Valley (Meltzer et al., 1995), fault striation analysis of Miocene rocks (Hippolyte et al., this volume; Mann et al., this volume), and marine geophysical surveying of faults offshore western Puerto Rico (Grindlay et al., this volume; Mann et al., this volume). The opposite sense of dip-slip observed in the trench relative to the decrease in the baseline length between PUR3 and PARG may arise from unmodeled signals in the relative velocities, such as seasonal effects, ocean loading and monument noise that yield potentially spurious results or may reflect changes in the local kinematics between the time of faulting and the present. We think it unlikely given the 6 yr time span and the consistency of other baseline measurements across Puerto Rico, however, that these results are unrelated to tectonic processes. For example, it has been demonstrated that velocity transients in GPS time series may be related to the earthquake cycle (Dragert et al., 2001). Although verification of such transients would require mechanical modeling to demonstrate their cause unequivocally, the possibility exists that the geodetically measured velocity field is recording strain accumulation related to the regional geodynamics of the plate boundary. Variations in the local strain field and the existence of additional unmapped structures between PARG and the Lajas Valley are other possible alternatives. Resolution of this discrepancy will require additional GPS geodetic data and a further analysis to remove regionally correlated noise. The campaign sites that span the Lajas Valley (LAJ1, LAJ2, and

LAJ3) (Fig. 2), which were first measured in early 2000, will provide critical constraints in the near future.

From Western to Eastern Puerto Rico: Distributed Deformation across the Island

The relative velocities and baseline evolution for GEOL-FAJA and PUR3-FAJA provide constraints on the overall deformation within and across Puerto Rico. GEOL-FAJA crosses both the Great Southern and Great Northern Puerto Rico fault zones, whereas PUR3-FAJA traverses only the latter (Fig. 2). The time interval considered is April 1999 until December 2001, reflecting when the site at Fajardo was installed. During this period, the baseline length between GEOL-FAJA increased by 3.9 ± 0.2 mm/yr (Fig. 6) (Table 2). The length change for PUR3-FAJA is smaller, but still positive at 1.5 ± 0.2 mm/yr, providing additional support for little displacement between GEOL and PUR3. While caution must be exercised when interpreting these data (see discussion above), the increasing baseline length and relative velocity (Fig. 5B) between fixed GEOL or fixed PUR3 and FAJA imply a component of approximately ENE-WSW–oriented extension of between 1.5 and 3.9 mm/yr across the island of Puerto Rico. Whether this extension is accommodated along a few major structures (e.g., the Great Northern Puerto Rico fault zone where the extension would generate dextral transtension) or distributed across several smaller features is not clear. Higher-than-average levels of seismicity do occur along the central segment of the Great Northern Puerto Rico fault zone (Asencio, 1980). The GPS-derived velocity relative to the Caribbean at ZSUA, a site between PUR3 and FAJA, is identical within error to that at FAJA, tentatively suggesting that the structures that take up displacement may be west of the San Juan metropolitan area. The errors associated with the GPS-derived velocities are still too large to conclude this definitively. We do note that there are several north-south–trending valleys that channel the major rivers along the north coast of Puerto Rico; these may be manifestations of east-west–oriented extension. One focal mechanism for the northwest corner of Puerto Rico is consistent with slip along north-south–striking normal faults (Fig. 1C). Hippolyte et al. (this volume) infer east-west extension across north-south–striking faults from fault striation studies in the Miocene carbonates of the northwestern corner of the island. The observation of likely ENE-WSW extension across Puerto Rico, therefore, is not surprising. Results from previous GPS studies and marine geophysical surveys document east-west extension between western Puerto Rico and eastern Hispaniola (van Gestel et al., 1998; Jansma et al., 2000; Calais et al., 2002). In addition, potential attachment of Virgin Gorda to the Caribbean at the eastern end of the Puerto Rico–northern Virgin Islands microplate requires near east-west extension between the eastern Virgin Islands and eastern Puerto Rico. In summary, the GPS geodetic data suggest that east-west extension is not limited to the offshore regions, but also likely affects the island of Puerto Rico at the level of 2–3 mm/yr. Orientations of T-axes from composite focal mechanisms also indicate east-west extension across eastern Puerto Rico (McCann, 2000).

From Eastern Puerto Rico and the Northern Virgin Islands to St. Croix and the Northern Lesser Antilles: Deformation across the Anegada Passage

The GPS-derived velocity relative to the Caribbean for FAJA in the northeastern corner of Puerto Rico is 2.0 ± 1.8 mm/yr (Fig. 5A and Table 1), which is very nearly no motion within error. We believe that no motion is unlikely and that after several more years of data accumulation the error estimate will likely decrease, yielding a small but statistically significant residual velocity. Evidence to support active slip in the region includes high seismicity (Frankel et al., 1980) and the occurrence in 1867 of a large ($7 < M < 7.75$) tsunamogenic earthquake along the north wall of the Virgin Islands basin that caused extensive damage in St. Croix and St. Thomas (Reid and Taber, 1920). To investigate potential motion across and along the Anegada passage in more detail, we examined the change in baseline length between FAJA in the northeastern corner of Puerto Rico and CRO1 on the island of St. Croix within the stable interior of the Caribbean plate. This has the advantage of eliminating the errors introduced by uncertainties in the Caribbean reference frame, related to variations in velocities among the five stable Caribbean sites. Baseline length increased at 1.9 ± 0.2 mm/yr (white noise; fit residuals) to 2.0 ± 2.3 mm/yr (relative velocities with errors propagated) (Table 2) in a direction perpendicular to the northeast-trending structures of the Whiting and Virgin Island basins, implying active extension across the Anegada passage, which is consistent with mapped structures in the offshore (Jany et al., 1987; Holcombe et al., 1989; Masson and Scanlon, 1991). A component of left-lateral strike-slip motion (1.2 ± 1.3 mm/yr) is also permissible within error from the baseline component and fixed site velocity analysis. This result is consistent given the westward-directed velocities of other sites in Puerto Rico (SALN, ADJN, PARG) relative to the Caribbean. A pair of focal mechanisms immediately south of the Anegada passage is consistent with left-lateral strike-slip faulting along east-west–oriented vertical planes (Fig. 1C).

From Western Puerto Rico to the Northeastern Dominican Republic: Opening of the Mona Rift

The new GPS observations from western Puerto Rico that incorporate 2000 and 2001 data are consistent with earlier results: velocities of sites in western Puerto Rico relative to the Caribbean remain significantly slower and more westerly trending (Fig. 5A) than velocities for sites in eastern Hispaniola (Fig. 2), implying ENE-WSW extension between the two islands. Comparing the total slip along major faults north and west of the Mona rift estimated from two-dimensional elastic models with the velocity of northwestern Puerto Rico, Jansma et al. (2000) inferred 5 ± 4 mm/yr extension across the Mona rift. New GPS geodetic data from the Dominican Republic and results

from three-dimensional elastic modeling of strain accumulation across Hispaniola and the immediate offshore region (Calais et al., 2002) lend additional support to near east-west extension of a few millimeters per year across the Mona rift.

Two major EW- to WNW-trending fault zones cut the island of Hispaniola: the Septentrional fault zone in the north and the Enriquillo fault zone in the south (Fig. 1B). The offshore continuation of the Septentrional fault projects to the South Puerto Rico Slope fault, which lies north of the Mona rift (Fig. 2) (Grindlay et al., 1997). Deformation also occurs immediately offshore Hispaniola to the north along the North Hispaniola deformed belt (Fig. 1B), a submarine zone of folds and thrusts, which was the locus of a series of large thrust earthquakes in 1946 and 1948 (Russo and Villaseñor, 1995; Dolan and Wald, 1998) and to the south along the Muertos trough. The Enriquillo fault disappears in central Hispaniola and slip in eastern Hispaniola may be transferred to the Muertos trough (Mann et al., 1999; Mauffret and Leroy, 1999). From their three-dimensional elastic model, Calais et al. (2002) estimate slip rates of 12.9 mm/yr, 9.0 mm/yr, 10.0 mm/yr, and 7.7 mm/yr along the North Hispaniola deformed belt, the Septentrional fault, the Enriquillo fault, and the Muertos trough, respectively. The 9 mm/yr rate for the Septentrional fault was constrained by Holocene rates derived from paleoseismological studies (Prentice et al., 2003). Their model is consistent with slip transfer from the Enriquillo fault to the Muertos trough south of eastern Hispaniola. If this is correct, GPS sites in central eastern Hispaniola are little affected by elastic strain accumulation, lying at substantially greater distance than the 15 km locking depth from the Septentrional fault and more than 100 km from the Muertos trough. GPS-derived velocities relative to the Caribbean of the central eastern Hispaniola sites are 3–5 mm/yr faster toward the WSW than the velocity at PARG (Calais et al., 2002), consistent with earlier estimates for opening across the Mona rift (Jansma et al., 2000).

CONCLUSIONS

Using GPS geodetic data collected throughout the northeastern Caribbean from 1994 until 2001, we are able to refine the velocities of Puerto Rico and the Virgin Islands with respect to the Caribbean plate, to constrain maximum permissible displacement rates along potentially active faults on the island of Puerto Rico and immediately offshore, and to examine potential diffuse extension between the Virgin Islands and eastern Puerto Rico. The existence of an independent Puerto Rico–northern Virgin Islands microplate was demonstrated at the 99.9% confidence level. At a location near the center of Puerto Rico (18.25°N, 66.5°W), motion of the Puerto Rico–northern Virgin Islands microplate with respect to the Caribbean is 2.6 ± 2.0 mm/yr (95%) directed toward N82.5°W ± 34° (95%). The geodetic data from the Puerto Rico–northern Virgin Islands block are consistent with east-west extension of several mm/yr in the boundary zone between the North America and Caribbean plates from eastern Hispaniola to the eastern Virgin Islands. The amount of extension increases westward with the most accommodated in the Mona rift between the Dominican Republic and western Puerto Rico, confirming earlier results from GPS geodesy. East-west extension of 1.5–3.9 mm/yr per year also potentially acts across the island of Puerto Rico. Whether this extension is localized along a few structures or is broadly distributed is unknown. We note that reactivation of the Great Northern and Great Southern Puerto Rico fault zones would yield oblique-normal slip with right-lateral sense along these structures. A zone of east-west extension of 1–2 mm/yr also must exist between eastern Puerto Rico and Virgin Gorda, which likely is attached to the Caribbean plate. These extensional belts allow eastward transfer of slip between North America and the Caribbean from the southern part of the plate boundary zone (Enriquillo fault in the southern Dominican Republic) to the northern (Puerto Rico trench offshore northern Virgin Islands). Increased seismicity in the Sombrero trend north of the northern and easternmost Virgin Islands is consistent with this interpretation.

The GPS-derived velocities of sites in Puerto Rico relative to the Caribbean, coupled with baseline changes and calculated relative velocities between selected stations, constrain maximum permissible displacement rates along active faults on the island and immediately offshore. Motions along or across any of the subaerial structures of Puerto Rico are ≤2 mm/yr. The Lajas Valley in the southwest, where microseismicity is greatest, is the locus of highest permissible on-land deformation. Northwest-southeast to east-west extension of 1.9 ± 0.2–2.0 ± 2.3 mm/yr across the Anegada Passage is also inferred from our GPS-derived velocities.

ACKNOWLEDGMENTS

This project could not have been completed without the support of numerous people: A. Eaby, A. Lopez, D. Martinez, H. Rodriguez, and S. Matson for assistance in data collection and E. Calais, C. DeMets, T. Dixon, and P. Mann for extensive discussions throughout the tenure of CANAPE. Thoughtful and comprehensive reviews by E. Calais and C. DeMets improved the final version of the manuscript. We also thank the Department of Marine Sciences, University of Puerto Rico, Mayagüez; the Agricultural Experiment Station in Isabela, Puerto Rico; the University of Puerto Rico, Humacao; B. Wiener; the Federal Aviation Administration Headquarters in San Juan, Puerto Rico; and the Guavaberry for continued access to their facilities. Work was supported by National Science Foundation grants EAR-9316215, EAR-9628553, EAR-9807289, EAR9806456, and HRD-9353549, National Aeronautics and Space Administration grant NCCW-0088, U.S. Geological Survey grant 01HQGR0041, and Puerto Rico Sea Grant award 535868.

REFERENCES CITED

Almy, C., Meltzer, A., and Dietrich, C., 2000, Faulting in the Lajas Valley and on the adjacent shelf, southwestern Puerto Rico: Eos (Transactions, American Geophysical Union), F1181.

Asencio, E., 1980, Western Puerto Rico seismicity: U.S. Geological Society Open-File Report, 80-192, p. 135.

Blewitt, G., Heflin, M.B., Webb, F.H., Lindqwister, U.J., and Malla, R.P., 1992, Global coordinates with centimeter accuracy in the International Terrestrial Reference Frame using GPS: Geophysical Research Letters, v. 19, p. 853–856.

Byrne, D.B., Suarez, G., and McCann, W.R., 1985, Muertos Trough subduction—Microplate tectonics in the northern Caribbean?: Nature, v. 317, p. 420–421.

Calais, E., Mazabraud, Y., Mercier de Lepinay, B., Mann, P., Mattioli, G., and Jansma, P., 2002, Strain partitioning and fault slip rates in the Caribbean from GPS measurements: Geophysical Research Letters, v. 29, no. 18, 1856, doi: 10.1029/2002G1015397.

DeMets, C., Jansma, P., Mattioli, G., Dixon, T., Farina, F., Bilham, R., Calais, E., and Mann, P., 2000, GPS geodetic constraints on Caribbean–North America plate motion: Implications for plate rigidity and oblique plate boundary convergence: Geophysical Research Letters, v. 27, p. 437–440, doi: 10.1029/1999GL005436.

Deng, J., and Sykes, L.R., 1995, Determination of Euler pole for contemporary relative motion of Caribbean and North American plates using slip vectors of interplate earthquakes: Tectonics, v. 14, p. 39–53, doi: 10.1029/94TC02547.

Dixon, T., G. Gonzales, E. Katsigris, and S. Lichten, 1991, First epoch geodetic measurements with the Global Positioning System across the northern Caribbean plate boundary zone: Journal of Geophysical Research, v. 96, p. 2,397–2,415.

Dixon, T.H., Farina, F., DeMets, C., Jansma, P., Mann, P., and Calais, E., 1998, Caribbean–North American plate relative motion and strain partitioning across the northern Caribbean plate boundary zone from a decade of GPS observations: Journal of Geophysical Research, v. 103, p. 15,157–15,182, doi: 10.1029/97JB03575.

Dolan, J.F., and Wald, D.J., 1998, The 1943–1953 north-central Caribbean earthquakes: active tectonic setting, seismic hazards and implications for Caribbean–North American plate motions, *in* Dolan, J., and P. Mann, eds., Active strike-slip and collisional tectonics of the northern Caribbean Plate boundary zone: Geological Society of America Special Paper 326, p. 143–161.

Dolan, J., Mullins, H., and Wald, D., 1998, Active tectonics of the north-central Caribbean: oblique collision, strain partitioning, and opposing subducted slabs, *in* Dolan, J., and Mann, P., eds., Active strike-slip and collisional tectonics of the northern Caribbean Plate boundary zone: Geological Society of America Special Paper 326, p. 1–61.

Dragert, H., Wang, K., and James, T., 2001, A silent slip event on the deeper Cascadia subduction interface: Science, v. 292, p. 1,525–1,528.

Erikson, J., Pindell, J., and Larue, D., 1990, Tectonic evolution of the south-central Puerto Rico region: Evidence for transpressional tectonism: Journal of Geology, v. 98, p. 365–368.

Erikson, J., Pindell, J., and Larue, D., 1991, Fault zone deformational constraints on Paleogene tectonic evolution in southern Puerto Rico: Geophysical Research Letters, v. 18, p. 569–572.

Frankel, A., McCann, W.R., and Murphy, A.J., 1980, Observations from a seismic network in the Virgin Islands region: Tectonic structures and earthquake swarms: Journal of Geophysical Research, v. 85, p. 2,669–2,678.

Glover, L., III, 1971, Geology of the Coama area, Puerto Rico and its relation to the volcanic arc-trench association: U.S. Geological Survey Professional Paper 636, p. 102.

Glover, L., III, and Mattson, P., 1960, Successive thrust and transcurrent faulting during the early Tertiary in south-central Puerto Rico: U.S. Geological Survey Professional Paper 400-B, 363–365.

Grindlay, N.R., Mann, P., and Dolan, J.F., 1997, Researchers investigate submarine faults north of Puerto Rico: Eos (Transactions, American Geophysical Union), v. 78, p. 404.

Heflin, M., Bertiger, W., Blewitt, G., Freedman, A., Hurst, K., Lichten, S., Lindqwister, U., Vigue, Y., Webb, F., Yunck, T., and Zumberge, J., 1992, Global geodesy using GPS without fiducial sites: Geophysical Research Letters, v. 19, p. 131–134.

Holcombe, T.L., Fisher, C.G., and Bowles, F.A., 1989, Gravity-flow deposits from the St. Croix Ridge; depositional history: Geo-Marine Letters, v. 9, p. 11–18.

Jansma, P., Mattioli, G., Lopez, A., DeMets, C., Dixon, T., Mann, P., and Calais, E., 2000, Neotectonics of Puerto Rico and the Virgin Islands, northeastern Caribbean from GPS geodesy: Tectonics, v. 19, p. 1021–1037.

Jany, I., Mauffret, A., Bouysse, P., Mascle, A., Mercier de Lépinay, B., Renard, V., and Stephan, J.F., 1987, Relevé bathymétrique Sea beam et tectonique en décrochement au sud des Iles Vierges (Nord-Est Caraibes): Comptes Rendus de l'Académie des Sciences, Serie II, Mecanique, Physique, Chimie, Sciences de l'Univers: Sciences de la Terre, v. 304, p. 527–532.

Joyce, J., McCann, W., and Lithgow, C., 1987, Onland active faulting in the Puerto Rico platelet: Eos (Transactions, American Geophysical Union), v. 68, p. 1,483.

Ladd, J.W., Worzel, J.L., and Watkins, J.S., 1977, Multifold seismic reflection records from the northern Venezuela Basin and the north slope of Muertos Trench, *in* Talwani, M., and Pitman, W.C., eds., Island arcs, deep-sea trenches and back-arc basins: Washington, D.C., American Geophysical Union, p. 41–56.

Ladd, J.W., and Watkins, J.S., 1978, Active margin structures within the north slope of the Muertos Trough: Geologie en Mijnbouw, v. 57, p. 225–260.

Langbein, J., and Johnson, H., 1997, Correlated errors in geodetic time series: implications for time-dependent deformation: Journal of Geophysical Research, v. 102, p. 591–603, doi: 10.1029/96JB02945.

Lao-Davila, D., Mann, P., Prentice, C., and Draper, G., 2000, Late Quaternary activity of the Cerro Goden fault zone, transpressional uplift of the La Cadena Range, and their possible relation to the opening of the Mona rift, western Puerto Rico: Eos (Transactions, American Geophysical Union), v. 81, p. F1181.

Larue, D.K., and Ryan, H.F., 1990, Extensional tectonism in the Mona Passage, Puerto Rico and Hispaniola: a preliminary study: Transactions of the Caribbean Geological Conference, v. 12, p. 301–313.

Larue, D.K., and Ryan, H.F., 1998, Seismic reflection profiles of the Puerto Rico Trench; shortening between the North American and Caribbean plates, *in* Lidiak, E.G., and Larue, D.K., eds., Tectonics and geochemistry of the northeastern Caribbean: Geological Society of America Special Paper 322, p. 193–210.

Lichten, S.M., 1990, Estimation and filtering for high precision GPS applications: Manual Geodesy, v. 15, p. 159–176.

Mann, P., Taylor, F., Edwards, L., and Ku, T., 1995, Actively evolving microplate formation by oblique collision and sideways motion along strike-slip faults: an example from the northeastern Caribbean plate margin: Tectonophysics, v. 246, p. 1–69, doi: 10.1016/0040-1951(94)00268-E.

Mann, P., McLaughlin, P., Jr., van den Bold, W., Lawrence, S., and Lamar, M., 1999, Tectonic and eustatic controls on Neogene evaporitic and siliciclastic deposition in the Enriquillo basin, Dominican Republic, *in* Mann, P., ed., Caribbean Basins, Sedimentary Basins of the World, 4: Elsevier: Amsterdam, p. 287–342.

Mann, P., Calais, E., Ruegg, J., DeMets, C., Jansma, P., and Mattioli, G., 2002, Oblique collision in the northeastern Caribbean from GPS measurements and geological observations, Tectonics, v. 21, no. 6, 1058, doi: 10.1029/2001TC001363.

Mao, A., Harrison, C.G.A., and Dixon, T.H., 1999, Noise in GPS coordinate time series: Journal of Geophysical Research, v. 104, p. 2,797–2,816.

Masson, D.G., and Scanlon, K.M., 1991, The neotectonic setting of Puerto Rico: Geological Society of America Bulletin, v. 103, p. 144–154, doi: 10.1130/0016-7606(1991)1032.3.CO;2.

Mauffret, A., and Jany, I., 1990, Collision et tectonique d'expulsion le long de la frontiere Nord-Caraibe: Oceanologica Acta, v. 10, p. 97–116.

Mauffret, A., and Leroy, S., 1999, Neogene intraplate deformation of the Caribbean plate at the Beata Ridge, *in* Mann, P., ed., Caribbean Basins, Sedimentary Basins of the World, 4: Elsevier: Amsterdam, p. 627–669.

McCann, W.R., 1985, On the earthquake hazards of Puerto Rico and the Virgin Islands: Bulletin of the Seismological Society of America, v. 75, p. 251–262.

McCann, W.R., 2002, Microearthquake data elucidate details of Caribbean subduction zone: Seismological Research Letters, v. 73, p. 25–32.

McCann, W.R., and Pennington, W.D., 1990, Seismicity, large earthquakes, and the margin of the Caribbean plate, *in* Dengo, G., and Case, J., eds., The Geology of North America, The Caribbean Region: Geological Society of America: Boulder, Colorado, Geology of North America, v. H, p. 291–306.

McCann, W. R., 2000, Characterization of active submarine faults near U.S. Caribbean territories: U.S. Geological Survey Final report for 99HQGR0067, 8 p.

Meltzer, A.S., Schoemann, M.L., Dietrich, C., Almy, C., and Schellekens, H., 1995, Characterization of faulting: southwest Puerto Rico: Geological Society of America Abstracts with Programs, v. 27, no. 6, p. 227.

Meltzer, A., 1997, Fault structure and earthquake potential of the Lajas Valley, SW Puerto Rico: U.S. Geological Survey Technical Abstract.

Mercado, A., and McCann, W., 1998, Numerical simulation of the 1918 Puerto Rico tsunami: Journal of Natural Hazards, v. 18, p. 57–76, doi: 10.1023/A:1008091910209.

Molnar, P., and Sykes, L.R., 1969, Tectonics of the Caribbean and Middle America regions from focal mechanisms and seismicity: Geological Society of America Bulletin, v. 80, p. 1639–1684.

Murphy, A.J., and McCann, W.R., 1979, Preliminary results from a new seismic network in the northeastern Caribbean: Bulletin of the Seismological Society of America, v. 69, p. 1497–1513.

Pacheco, J.F., and Sykes, L.R., 1992, Seismic moment catalog of large shallow earthquakes, 1900 to 1989: Bulletin of the Seismological Society of America, v. 82, p. 1306–1349.

Prentice, C., Mann, P., Peña, L., and Burr, G., 2003, Slip rate and earthquake recurrence along the central Septentrional fault, North American–Caribbean plate boundary, Dominican Republic: Journal of Geophysical Research, v. 108(B3), 2149, doi: 10.1029/2001JB00042.

Prentice, C., Mann, P., and Burr, G., 2000, Prehistoric earthquakes associated with a Late Quaternary fault in the Lajas Valley, southwestern Puerto Rico: Eos (Transactions, American Geophysical Union), v. 81, p. F1182.

Reid, H., and Taber, S., 1920, The Virgin Islands earthquakes of 1867–1868: Bulletin of the Seismological Society of America, v. 10, p. 9–30.

Reid, J., Plumley, P., and Schellekens, J., 1991, Paleomagnetic evidence for late Miocene counterclockwise rotation of the North Coast carbonate sequence, Puerto Rico: Geophysical Research Letters, v. 18, p. 565–568.

Russo, R.M., and Villaseñor, A., 1995, The 1946 Hispaniola earthquake and the tectonics of the North America–Caribbean plate boundary zone, northeastern Hispaniola: Journal of Geophysical Research, v. 100, p. 6,265–6,280.

Stein, S., and Gordon, R.G., 1984, Statistical tests of additional plate boundaries from plate motion: Earth and Planetary Science Letters, v. 69, p. 401–412, doi: 10.1016/0012-821X(84)90198-5.

Sykes, L.R., McCann, W.R., and Kafka, A.L., 1982, Motion of Caribbean plate during last 7 million years and implications for earlier Cenozoic movements: Journal of Geophysical Research, v. 87, p. 10,656–10,676.

van Gestel, J., Mann, P., Dolan, J., and Grindlay, N., 1998, Structure and tectonics of the upper Cenozoic Puerto Rico–Virgin Islands carbonate platform as determined from seismic reflection studies: Journal of Geophysical Research, v. 103, p. 30,505, doi: 10.1029/98JB02341.

Ward, S.N., 1990, Pacific–North America plate motions: new results from very long baseline interferometry: Journal of Geophysical Research, v. 95, p. 21,965–21,981.

Weber, J.C., Dixon, T., DeMets, C., Ambeh, W.B., Jansma, P., Mattioli, G., Saleh, J., Sella, G., Bilham, R., and Pérez, O., 2001, A GPS estimate of relative motion between the Caribbean and South American plates and geologic implications for Trinidad and Venezuela: Geology, v. 29, p. 75–78, doi: 10.1130/0091-7613(2001)0292.0.CO;2.

Zumberge, J.F., Heflin, M., Jefferson, D., Watkins, M., and Webb, F., 1997, Precise point positioning for efficient and robust analysis of GPS data from large networks, Journal of Geophysical Research, v. 102, p. 5,005–5,017.

Manuscript Accepted by the Society 18 August 2004

Printed in the USA